

A ONE-PHASE DUAL CONVERTER FOR TWO QUADRANT POWER CONTROL OF SUPERCONDUCTING MAGNETS\*

M. Ehsani  
Senior member, IEEE  
Electrical Engineering  
Texas A&M University  
College Station, Texas 77843

R. L. Kustom  
Member IEEE  
Physics Division  
Argonne National Laboratory  
Argonne, Illinois 60439

R. W. Boom  
Senior member, IEEE  
Applied Superconductivity Center  
University of Wisconsin  
Madison, Wisconsin 53706

Abstract

This paper presents the results of theoretical and experimental development of a new dc-ac-dc converter for superconducting magnet power supplies. The basic operating principles of the circuit are described followed by a theoretical treatment of the dynamics and control of the system. The successful results of the first experimental operation and control of such a circuit are presented and discussed.

Introduction

Superconductive magnet coils are being increasingly used for energy storage and generation of high magnetic fields in research and industry. Examples of superconductive energy storage magnets under study or in operation are Wisconsin Superconductive Energy Storage coil<sup>1</sup> and the Los Alamos National Laboratory experimental power system stabilizer coil<sup>2</sup>. Examples for magnetic field generation are the equilibrium field (EF) coils of Argonne National Laboratory proposed Tokamak Experimental Power Reactor<sup>3</sup> and the Tevatron magnets of Fermi National Laboratory accelerator.<sup>4</sup>

From the electrical terminals, the superconductive coil is a virtually resistance-free large inductor, capable of storing large amounts of energy. To supply this energy efficiently, the power supply should also have low losses and be capable of reversible power control. This is particularly important in repetitively energized magnets. Solid state switching power supplies have been utilized for this purpose in recent years (Figure 1 (a)). Low conduction and switching losses at high frequencies and the increasing power ratings of solid state switches make solid state switching supplies favorable for superconductive magnet applications onto the future.

Where repetitive bidirectional (two-quadrant) power control is required, power supply circuits using another superconductive energy storage coil as a buffer have been suggested<sup>5,6,7,8</sup>. The main advantage these circuit arrangements (Figure 1(b)) is that high power oscillations, required by the load, are supplied by the energy storage coil. Thus, a relatively small power generator or utility link can be used for the initial charging of the storage coil and also for system loss compensation in a steady state. Two examples of power supplies with energy storage buffer are the flying capacitor<sup>6</sup> arrangement and the inductor-converter bridge<sup>5</sup> (ICB). A study of several of these circuits has been presented in reference 7.

This paper presents the results of theoretical and experimental work on a new one-phase dual converter for magnet supply which is in the class of ICB circuits.

The One-Phase Inductor-Converter Bridge

In this section we will describe the operation of the one-phase ICB and analyze its dynamic behavior. A more complete presentation of this subject appears in reference 9.

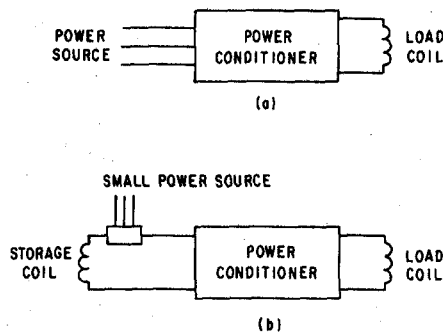


Figure 1 Two power supply arrangements for pulsed inductive loads.

Circuit Operation

Figure 2 shows a schematic diagram of the circuit. The load magnet,  $L_L$ , and the storage magnet,  $L_S$ , are each connected to a full wave one-phase converter. The ac lines of the two converters are connected in parallel with the capacitor,  $C$ . The switching sequence on the storage converter is  $S_{11}S_{14}, S_{12}S_{13}, S_{11}S_{14}$ , etc. Similar switching sequence and frequency is used on the load converter. However, a leading switching timing of the load converter, relative to the storage converter, will cause a net energy transfer from storage to load coil, and vice versa. The capacitor,  $C$ , temporarily stores the energy which is transferred from one coil to the other in each converter cycle. The switching frequency of the converters is so high that only an infinitesimal fraction of the system energy is stored in the capacitor at any one time. Therefore, the capacitive energy storage requirement of the system is very low.

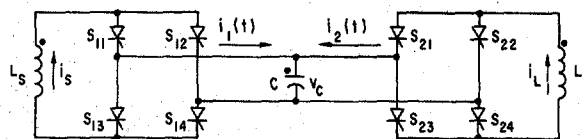


Figure 2 Circuit diagram of the one-phase ICB.

The capacitor also supplies the commutation voltages to the converters. Commutation between  $S_1S_4$  and  $S_2S_3$  conduction patterns on each converter produces an instantaneous double short circuit across each coil. The impedance of the commutation loops; e.g.,  $C - S_{11} - S_{12}$ , is kept so low that even a small capacitor voltage of the correct polarity will drive sufficient commutation current in the loop. Two such commutation instants occur on each converter, per cycle. Note that a commutation failure is inherently safe because the double short circuits of the failed converter serve as safety crowbars across the corresponding coil.

\* Work supported by the U.S. Department of Energy and Applied Superconductivity Laboratory of University of Wisconsin. Manuscript received September 10, 1984.

The circuit usually begins operation with the storage inductor fully charged and the load inductor uncharged. The capacitor may be precharged, for example to a negative voltage for  $S_1S_4$  initial switching in each converter. Thereafter, proper operation will insure the availability of the correct commutation voltage polarities.

Circuit Dynamic Analysis

Figure 3 shows an idealized model of the one-phase ICB in which the SCR's are replaced by ideal switches. Because of high frequency, the coil currents do not change significantly in a converter cycle of interest and may be represented by constant current sources,  $I_S$  and  $I_L$ . The switching action of the converters produces square wave ac current  $i_1$  and  $i_2$  from the coil currents  $I_S$  and  $I_L$ . Each constant current source and its converter may be replaced by its equivalent ac current source function,  $i_1$  and  $i_2$ , resulting in the circuit of Figure 4. The capacitor is left unchanged. An example of  $i_1$  and  $i_2$  current waveforms is shown in Figure 7.

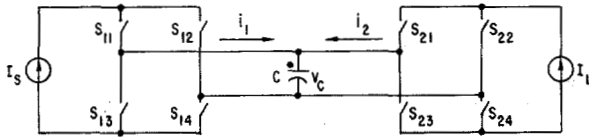


Figure 3 Idealized circuit model of the one-phase ICB.

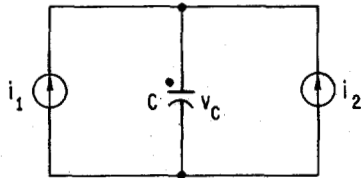


Figure 4 Equivalent circuit model of the one-phase ICB.

The average power from one source to the other, in Figure 4, may be calculated over one cycle. However, since  $i_1$  and  $i_2$  are square waves the calculation may be done on their Fourier components. This calculation is shown in reference 9 and the resulting expression is

$$\langle p_S \rangle = \sum_{n=1}^{\infty} \frac{4I_S I_L}{n^3 \pi^2 \omega C} [1 - (-1)^n] \sin n\phi, \quad (1)$$

where  $\langle p_S \rangle$  is average storage coil output power over one cycle,  $I_S$  and  $I_L$  are the average coil currents over the same cycle,  $\omega$  is the angular frequency of the converters, and  $\phi$  is the load converter advance angle. A closed form for  $\langle p_S \rangle$  may be derived if  $i_1, i_2$  and  $v_C$  are expressed in terms of a new set of orthogonal switching functions<sup>9</sup>. The result is

$$\langle p_S \rangle = \frac{I_S I_L}{\omega C} (\phi - \phi^2/\pi) \quad (2)$$

a plot of  $\langle p_S \rangle$  vs. the control angle,  $\phi$ , is shown in Figure 5. Note that the instantaneous power can be controlled from zero to its maximum value as  $\phi$  is varied from zero to  $90^\circ$ .

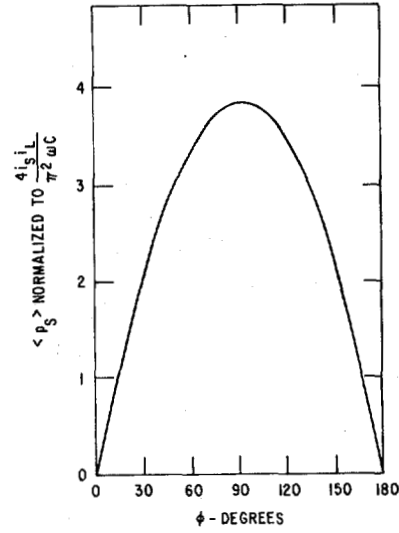


Figure 5 Average power vs. control angle in one-phase ICB.

Since the ideal ICB is lossless, the instantaneous coil currents, averaged over a cycle,  $i_S \triangleq I_S$  and  $i_L \triangleq I_L$ , can be derived from differential equations based on conservation of power:

$$\text{storage output power} = \langle p_S \rangle = -\frac{d}{dt} \left( \frac{1}{2} L_S i_S^2 \right), \quad (3)$$

$$\text{load input power} = \langle p_S \rangle = \frac{d}{dt} \left( \frac{1}{2} L_L i_L^2 \right), \quad (4)$$

$$i_S(0) = I_o = \text{initial storage current}, \quad (5)$$

$$L_L \frac{di_L}{dt} \Big|_{t=0} = 0 = \text{initial load voltage} \quad (6)$$

substituting for  $\langle p_S \rangle$  from eq. (2), and solving the differential equations, the coil current expressions as a function of time are

$$i_S(t) = I_o \cos \frac{k}{\sqrt{L_S L_L}} t, \quad (7)$$

$$i_L(t) = I_o \sin \frac{k}{\sqrt{L_S L_L}} t, \quad (8)$$

where

$$k \triangleq (\phi - \phi^2/\pi)/\omega C. \quad (9)$$

The instantaneous coil power, averaged over a cycle ( $p_S \triangleq \langle p_S \rangle$ ), is found by substituting equations (7) and (8) in eq. (2):

$$P_S(t) = \frac{1}{2} k I_o^2 \sqrt{L_S/L_L} \sin \frac{2k}{\sqrt{L_S L_L}} t. \quad (10)$$

The instantaneous coil voltages, averaged over a cycle,  $v_S$  and  $v_L$ , are found from  $v = L di/dt$ . The results are

$$v_S(t) = k I_o \sqrt{L_S/L_L} \sin \frac{k}{\sqrt{L_S L_L}} t, \quad (11)$$

$$v_L(t) = k I_o \sqrt{L_S/L_L} \cos \frac{k}{\sqrt{L_S L_L}} t, \quad (12)$$

Equations (7), (8), (10), (11) and (12) indicate the effect of the control angle,  $\phi$ , on the dynamic behavior of the circuit.

Load Current Control

The one-phase ICB is not only intended for charging and discharging of a load magnet but also for real time control of the load magnetic field based on an arbitrary reference signal. For load magnetic field control a bang-bang or maximum effort control strategy has been devised which provides a time optimal response to step reference changes. This microcomputer based algorithm acquires the present value of load current,  $i_L(t_k)$ , reference current  $i_r(t_k)$  and control angle  $\phi(t_k)$ . If  $i_L(t_k) < i_r(t_k)$ , a next value of control angle,  $\phi(t_{k+1})$  for maximum power to the load is issued. Conversely, if  $i_L(t_k) > i_r(t_k)$  a next value of control angle for maximum power from the load is issued. The control angle is unchanged if  $i_L(t_k) = i_r(t_k)$ . The control angle for maximum positive and negative power can be obtained by differentiating eq. (2). These values which are also evident from Figure 6, are  $\phi = 90^\circ$  for positive power to the load and  $\phi = -90^\circ$  for negative power. Equation (2) shows that converter frequency,  $\omega$ , can also control the load power. However,  $\omega$  is usually based on other design constraints and will not be considered for control in this paper.

The above control strategy operates the load converter at either  $90^\circ$  lead or lag, relative to the storage converter, at all times.

Methods of Phase Shifting

Bang-Bang control strategy requires frequent  $180^\circ$  phase shifting between  $90^\circ$  and  $-90^\circ$ . Phase shifts are implemented by shortening or lengthening the switching time intervals on one or both converters of the ICB. Such switching interval perturbations can introduce bias voltages on the capacitor which can result in commutation or over voltage failures. A systematic method of phase shifting without producing any voltage bias is described below.

To cause a load converter lead, relative to the storage converter of the ICB, its switching intervals are temporarily shortened. This temporary alteration of the switching is called a transient switching sequence and is then followed by the equal interval switching sequence. The shortest phase shifting transient switching sequence which will not introduce a capacitor voltage bias is a three-step sequence. If the steady state switching interval on each converter is  $\Delta t$ , the three transient intervals,  $\Delta t_1, \Delta t_2$  and  $\Delta t_3$  are derived from

$$\Delta t_1 = \Delta t - \frac{\Delta t_\phi}{2}, \tag{13}$$

$$\Delta t_2 = \Delta t - \frac{\Delta t_\phi}{2}, \tag{14}$$

$$\Delta t_3 = \Delta t, \tag{15}$$

where  $\Delta t_\phi$  is the time shift corresponding to  $\phi$  degrees of converter phase shift. Figure 6 shows typical waveforms of a three-step switching sequence which delays the load converter by  $90^\circ$ . The  $180^\circ$  phase shifts, required by the bang-bang control algorithm, can also be implemented in three transient intervals. However, in our experiments the  $180^\circ$  shifts were done in two consecutive three-step sequences. This provided additional margin of commutation voltages on the capacitor. Figure 7 shows the graphical derivation of capacitor waveform during a typical  $180^\circ$  shift when  $i_S < i_L$ .

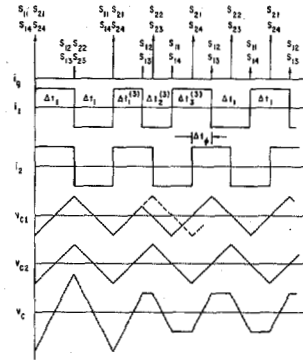


Figure 6 Transient switching sequence for phase shifting of  $\phi = 0^\circ \rightarrow -90^\circ$  when  $i_L/i_S = 1$ .

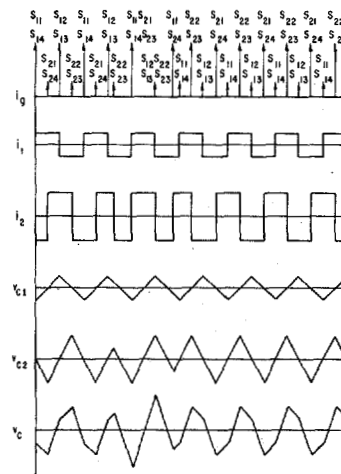


Figure 7 A  $180^\circ$  phase shift in two  $90^\circ$  segments:  $(-90^\circ \rightarrow 0 \rightarrow 90^\circ)$ .

Proper commutation voltage polarity on the capacitor also depends on the control angle,  $\phi$ . The one-phase ICB will fail to commutate if operated beyond the safe control angle thresholds shown in Figure 8. This figure shows that the safe thresholds are  $\phi = \pm 90^\circ$  at the beginning of the transfer,  $i_L/i_S = 0$  and increases to  $\pm 180^\circ$  at  $i_L/i_S = 1$ , then decreases back to  $90^\circ$  as the entire energy is transferred to the load  $i_S/i_L = 0$ . Therefore, bang-bang control strategy, which operates within  $-90^\circ \leq \phi \leq 90^\circ$ , will always commutate successfully.

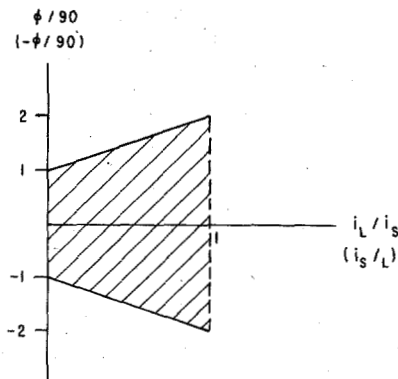


Figure 8 Plot of safe control phase thresholds.

### Experimental Results

A small experimental one-phase ICB was built to verify the operation and control methods described in this paper. Some important specifications of the circuit are listed in table 1.

Table 1, Experimental Circuit Specifications

$$L_S = L_L = 4H$$

$$I_o = 100A$$

$$C = 2.5 \times 10^{-4}F$$

$$W = 6233\text{rad/S}$$

rated coil energy = 125KJ  
rated converter power = 2.5KW

Several circuit tests at constant control angles established the practicality of the one-phase ICB concept and also the soundness of the experimental circuit design. Figure 9 shows the load coil currents through one complete energy transfer from  $L_S$  to  $L_L$ . Note that the falling  $i_S$  and the rising  $i_L$  follow equations (7) and (8), respectively. Only the first quarter cycle of these equations are valid in describing the coil currents. The final load coil current is somewhat smaller than the initial storage current because of system losses which were not minimized in these tests. A series of bang-bang control experiments were conducted to verify the transient switching techniques. The system behaved in accordance with the prediction. An example of the capacitor voltage during a phase shift of  $\phi = 90^\circ$  to  $-90^\circ$  is shown in Figure 10. This waveform is to be compared with  $v_c$  in Figure 7 which was drawn for the same  $i_L/i_S$  state.

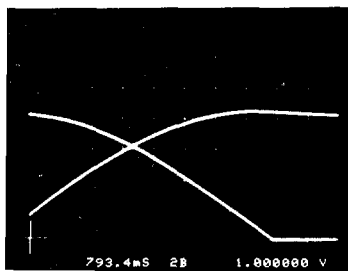


Figure 9 Coil current waveforms through a full energy transfer at  $\phi = 60^\circ$ .

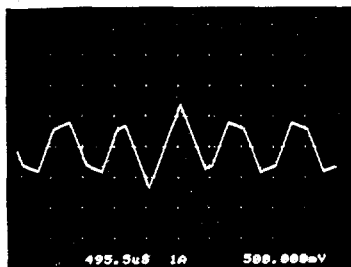


Figure 10 Capacitor voltage during a  $\phi = 90^\circ \rightarrow -90^\circ$  phase shift.

### Conclusions

The experiments with the one-phase ICB established that this circuit is a practical alternative for superconducting magnet power supply. The most important advantages of this circuit are its simplicity of topology and its control. Compared to the other ICB's this circuit has fewer switching elements in its topology. From the

complexity and reliability point of view this can mean smaller number of snubbers, gate drives, and similar switching and protection auxiliary equipment. From the control point of view the one-phase ICB has a binary switching pattern on each converter which is the simplest pattern to implement by software or discrete electronics. Furthermore, the phase shifting transient switching sequences of the one-phase ICB are simpler than the three-phase ICB<sup>10</sup>. This can also simplify the control software and electronics.

Another characteristic of the one-phase ICB is its converter switch utilization factor of 50 % per cycle. This factor for the three-phase ICB is 33 % . This can translate into a reduction in the total number of SCR's needed by the one-phase ICB in high current applications.

Finally, the experiments on the one-phase ICB proved this circuit to be remarkably resilient to capacitor voltage errors and commutation failures. This circuit, augmented by the robust bang-bang control strategy, makes an attractive design option for repetitively pulsed large magnet power supplies.

### References

1. R. W. Boom, H. A. Peterson, et. al., Wisconsin Superconductive Energy Storage Project Report, Vol. I, July 1984.
2. J. F. Haver and H. J. Boenig, "Electrical Tests of 30 MJ Superconducting Magnet Energy Storage System within the Bonneville Power Administration Power Grid," Los Alamos National Laboratory Report LA-UR-2574, September, 1983.
3. Tokamak Experimental Power Reactor Conceptual Design, Argonne National Laboratory Report ANL/CTR-76-3, 1976.
4. A. D. McInturff, et. al., "High Field Accelerator Magnet Design (10T, 2T/cm), Material and Model Development," *IEEE Trans. on Nucl. Sci.*, Vol. NS30, No. 4, Aug. 1983.
5. H. A. Peterson, N. Mohan, W. C. Young, and R. W. Boom, "Superconductive Inductor Converter Units for Pulsed Power Loads," *Proc. of Int. Conf. on Energy Storage, Compression, and Switching*, Asti-Torino, Italy, Nov. 1974.
6. E. P. Dick and H. Dustman, "Inductive Energy Transfer using a Capacitor," *Proc. of Int. Conf. on Energy Storage, Compression, and Switching*, Asti-Torino, Italy, Nov. 1974.
7. R. L. Kustom, Thyristor Networks for the Transfer of Energy Between Superconducting Coils, University of Wisconsin Press, 1980.
8. H. L. Laquer, F. L. Ribe, and D. M. Wilson, "Energy Storage and Switching with Superconductors as a power source for Magnetic Fields in pulsed Thermonuclear Experiments and Reactors," *Intersociety Energy Conversion Engineering Conf.*, Boston, MA, Aug. 1971.
9. M. Ehsani and R. L. Kustom, "A New One-Phase Dual Converter for Superconducting Inductive Energy Storage and Transfer Applications: The One-Phase Inductor-Converter Bridge, Argonne, National Laboratory Report ANL/FPP/TM-182, 1984.
10. M. Ehsani and R. L. Kustom, Development, Analysis, and Control of the Inductor-Converter Bridge, Argonne National Laboratory Report, ANL/FPP/TM-144, 1981.